PROCEEDINGS

International Workshop on Astroparticle and High Energy Physics

Solar neutrinos: What is next?

Alexei Smirnov*

International Centre for Theoretical Physics
strada Costiera 11, 34014 Trieste, Italy
E-mail: smirnov@ictp.trieste.it

Abstract: Status of the solar neutrino studies after KamLAND and the SNO salt phase experiment is summarized. The present data determine quantitatively the physical picture of the solar neutrino conversion. The next step in the field will be related to further checks of the LMA MSW solution, precision measurements of the oscillation parameters, searches for sub-leading effects and studies of solar neutrino fluxes. The predictions for the forthcoming measurements are given which include the spectral distortion and CC/NC ratio at SNO, the Day-Night asymmetry, the KamLAND spectrum and rate. The Homestake result is about $\sim 2\sigma$ lower than the Ar-production rate, Q_{Ar}, predicted by the LMA MSW solution. Also there is no apparent "upturn" of the energy spectrum ($R \equiv N_{obs}/N_{SSM}$) at low energies in SNO and Super-Kamiokande. Both these facts can be explained if a light sterile neutrino exists which mixes very weakly with active neutrinos. Future studies of the solar neutrinos by SNO, SK, BOREXINO and KamLAND as well as by the new low energy experiments will allow us to check this possibility. In connection to future precision measurements of the solar neutrino fluxes effects of the non-zero 13-mixing are considered.

This text is based on the papers hep-ph/0307266 and hep-ph/0309299 written in collaboration with P.C. de Holanda.

Dedicated to Jose who knows why we are writing proceedings...

1. After SNO salt results

The SNO-II (salt phase) results [1] have further confirmed correctness of both the neutrino fluxes predicted by the Standard Solar Model (SSM) [2] and picture of the solar neutrino conversion based on the MSW effect [3, 4]. Together with the results from the SNO phase-I [5], Homestake [6], SAGE [7], GALLEX [8], GNO [9] and Super-Kamiokande [10, 11] experiments as well as from the reactor experiment KamLAND [12] the latest SNO results

*Speaker.

lead to better determination of the oscillation parameters. This improvement allows one to make two important qualitative statements [1]:

- the h-LMA region, which corresponds to $\Delta m^2 > 10^{-4}$ eV^2, is strongly disfavored (being accepted at the 3σ level);
- there is a substantial deviation of 1-2 mixing from the maximal one, and the latter is rejected by more than 5σ standard deviations.

These statements have been confirmed by followed analyzes [13, 14, 15, 16, 17, 18]. After the SNO-II measurements, physics of the solar neutrino conversion is essentially determined. In particular, relative contributions of the adiabatic conversion in matter and the oscillation effect for different energies can be quantified.

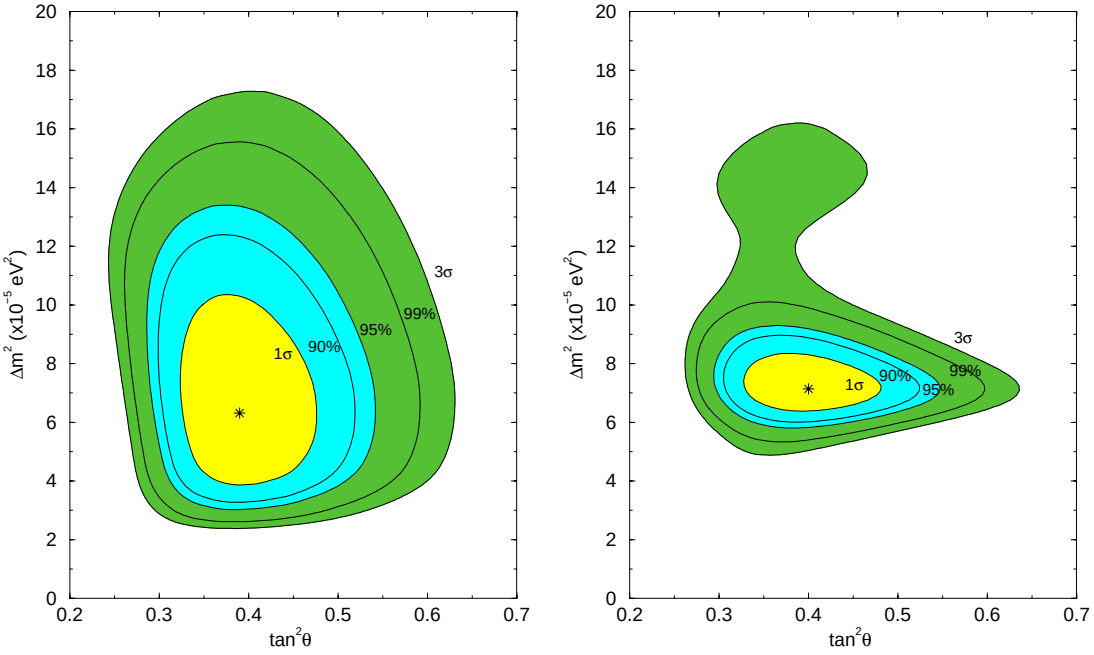

Figure 1: The allowed regions in $\tan^2\theta - \Delta m^2$ plane, from a combined analysis of the solar neutrino data (left) and from a combined analysis of the solar neutrino data and the KamLAND spectrum at 1σ, 90%, 95%, 99% and 3σ C.L.. The boron neutrino flux is treated as free parameter. The best fit point is marked by star.

Results of analysis of the solar and KamLAND data are shown in fig. 1. Details can be found in [19] and in our previous publications [20, 21]. All the solar neutrino fluxes, but the boron neutrino flux, are taken according to SSM BP2000 [2]. The boron neutrino flux measured in the units of the Standard Solar Model flux [2], $f_B \equiv F_B/F_B^{SSM}$, is treated as a free parameter.

The minimum, $\chi^2_{sun}(min)/d.o.f. = 67/81$ is achieved at

$$\Delta m^2 = 6.31 \cdot 10^{-5}\text{eV}^2, \quad \tan^2\theta = 0.39, \quad f_B = 1.063. \tag{1.1}$$

From the pre-salt analysis we had: $(\Delta m^2, \tan^2\theta) = (6.15 \cdot 10^{-5}, 0.41)$ [21]. So, the SNO-II data only slightly shifted the best fit point to smaller values of Δm^2 and $\tan^2\theta$. The boron neutrino flux was smaller: $f_B = 1.05$.

Assuming CPT conservation one can perform a combined fit of the solar neutrino data and KamLAND spectral results. We calculate the global χ^2

$$\chi^2_{global} \equiv \chi^2_{sun} + \chi^2_{KL} \ . \tag{1.2}$$

The absolute minimum, $\chi^2_{global}(min)/d.o.f. = 73.4/94$ is at

$$\Delta m^2 = 7.13 \cdot 10^{-5}\mathrm{eV}^2, \quad \tan^2\theta = 0.40, \quad f_B = 1.038. \tag{1.3}$$

From fig. 1 we get the following upper bounds on mixing:

$$\tan^2\theta < \begin{cases} 0.48, & 1\sigma \\ 0.55, & 2\sigma \\ 0.64, & 3\sigma \end{cases} . \tag{1.4}$$

Maximal mixing is excluded at 5.2σ. These bounds follow from the solar neutrino data being practically unaffected by KamLAND. The 1-2 mixing deviates substantially from the maximal one:

$$(\sin^2\theta - 0.5) \sim \sin^2\theta. \tag{1.5}$$

2. Physics of the solar neutrino conversion.

With new SNO results the h-LMA region is excluded or strongly disfavored and also significant deviation of 1-2 mixing from maximum is established. This essentially determines both qualitatively and now quantitatively the physical picture of solar neutrino conversion (see also [22]).

We take the difference of the matter potentials for ν_e and ν_a (active) according to the Standard Model:

$$V = \sqrt{2} G_F \rho Y_e / m_N. \tag{2.1}$$

Here ρ is the matter density, Y_e is the number of electrons per nucleon, and m_N is the nucleon mass. In fact, the latest experimental data allow to check the presence of such a potential in the model independent way. The extracted value of the potential is in agreement with (2.1) (within 1σ) and $V = 0$ is rejected at $\sim 5.6\sigma$ level [14].

For parameters (1.3) the neutrino evolution inside the Sun occurs in the highly adiabatic regime. It is convenient to write the averaged adiabatic survival probability as [3, 4]

$$P = \sin^2\theta + \cos 2\theta \ \cos^2\theta^0_m, \tag{2.2}$$

where θ^0_m is the mixing angle in the production point. Provided that there is no coherence lost (see discussion at the end of the section), the depth of oscillations at the surface of the Sun equals [4]

$$A_P = \sin 2\theta \sin 2\theta^0_m. \tag{2.3}$$

So that the probability (being the oscillatory function of distance) is inscribed in the following oscillation strip

$$P \pm \frac{1}{2} \sin 2\theta \sin 2\theta^0_m. \tag{2.4}$$

The oscillation length in matter, l_m, is smaller than the resonance oscillation length, $l_R \equiv l_\nu / \sin 2\theta$, where l_ν is the vacuum oscillation length. So, for typical energy 10 MeV we find $l_m \sim 3.5 \cdot 10^7$ cm. Along the solar radius, $R_\odot$, about $R_\odot / l_m \sim 2 \cdot 10^3$ oscillation length are obtained, and consequently, the oscillations are strongly averaged out.

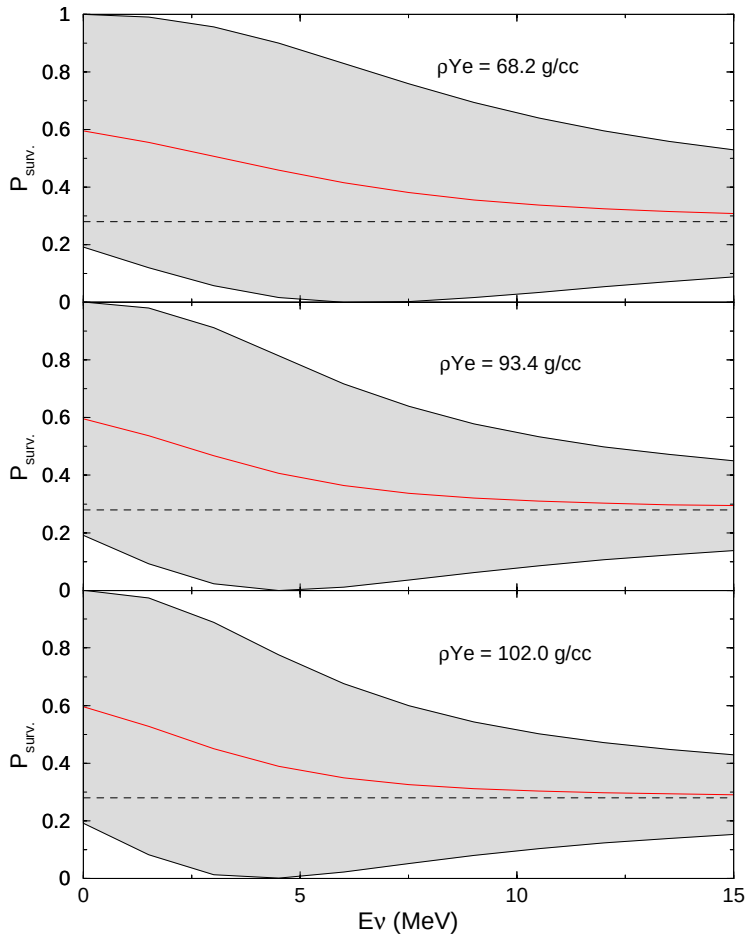

Figure 2: The averaged survival probability as a function of the neutrino energy for different production initial densities ρY_e. The oscillation strips (shadowed) show the depth of oscillations at the surface of the Sun. The non-oscillatory conversion probability $P_{non-osc} = \sin^2\theta$ is shown by the dashed line.

Dynamics of the effect depends on $\sin^2\theta$ and

$$\eta(E) \equiv \frac{E_{kin}}{V_0} = \frac{\Delta m^2}{2EV_0} = \frac{\Delta m^2 m_N}{2\sqrt{2}EG_F(\rho Y_e)_0}, \tag{2.5}$$

which is the ratio of the "kinetic" energy, $\Delta m^2/2E$, and the potential energy in the neutrino production point, V_0. For a given energy, η determines the relative contributions of the vacuum oscillation and the matter effect.

Depending on η there are two limits:

1. Matter dominance: $\eta \ll 1$ which corresponds to $E \to \infty$. In this limit the neutrino flavor evolution has a character of the non-oscillatory ($A_P = 0$) conversion with the survival

probability [4]:

$$P_{non-osc} = \sin^2\theta. \tag{2.6}$$

In this case neutrinos produced far above the resonance density propagate to zero (small) density adiabatically. The initial mixing is strongly suppressed ($\theta^0_m \approx \pi/2$) and the propagating neutrino state practically coincides with the heaviest eigenstate: $\nu(t) = \nu_{2m}$. At the exit from the Sun: $\nu(t) = \nu_2$ [4].

2. Vacuum dominance: $\eta \gg 1$ which corresponds to $E \to 0$. Matter effects are small. The flavor evolution has a character of vacuum oscillations, so P converges to the averaged oscillation probability

$$P \to P_{vac} = 1 - 0.5\sin^2 2\theta, \tag{2.7}$$

and $A_P \to \sin^2 2\theta$.

For the reference value of mixing (1.3) we find

$$P_{non-osc} = 0.281, \qquad P_{vac} = 0.596. \tag{2.8}$$

The resonance value of η, for which $P = 1/2$, equals

$$\eta_R = \frac{1}{\cos 2\theta} = 2.28. \tag{2.9}$$

It marks the transition region between the two extreme cases.

The ratio CC/NC measured by SNO determines the survival probability averaged over the energy range above the SNO threshold for the CC events ($E \sim 5$ MeV):

$$\frac{\text{CC}}{\text{NC}} = \langle P \rangle. \tag{2.10}$$

For the reference value (1.3) we get $\langle P \rangle = 0.322$. This value is slightly larger than the experimental result.

So, both the experimental and theoretical values of CC/NC are rather close to $P_{non-osc}$ which means that at high energies ($E > 5$ MeV) the evolution of neutrino state is nearly non-oscillatory conversion. The difference

$$\frac{\text{CC/NC}}{P_{non-osc}} - 1 = \frac{\text{CC/NC}}{\sin^2\theta} - 1 = 0.13 \tag{2.11}$$

is due to

- the averaged oscillation effect inside the Sun. In fact, for $(\rho Y_e)_0 \approx 93.4$ g/cc and energies relevant for the SNO CC signal, $E = 14, 10, 6$ MeV, we obtain $\eta = 0.36, 0.50, 0.84$ correspondingly. These values of η are not small, though being smaller than the resonance value. Therefore one may expect a significant deviation of P from the asymptotic value.

- the earth regeneration effect.

The survival probability can be written as

$$P = \sin^2\theta + \Delta P_{reg} + \Delta P_{osc}, \tag{2.12}$$

where ΔP_{reg} is the regeneration correction and ΔP_{osc} is the oscillation correction. Both these corrections are positive.

The regeneration effect, ΔP_{reg}, can be expressed in terms of the Day-Night asymmetry, A_{DN}, as:

$$\Delta P_{reg} \approx A_{ND} \cdot P_{non-osc} \approx \sin^2\theta \cdot A_{ND}. \tag{2.13}$$

For the best fit point the asymmetry equals $A_{ND} = 3.0\%$, and consequently, $\Delta P_{reg} = 0.008$.

Using formula for the adiabatic conversion (2.2) we find:

$$\Delta P_{osc} = \cos 2\theta \cos^2\theta^0_m. \tag{2.14}$$

In the limit of small η we find

$$\cos^2\theta^0_m \approx \frac{1}{4}\sin^2 2\theta\ \eta^2, \tag{2.15}$$

and therefore the correction to probability can be written as

$$\Delta P_{osc} = \frac{1}{4}\cos 2\theta \sin^2 2\theta\ (\eta^2 + O(\eta^3)). \tag{2.16}$$

Notice that the correction is quadratic in η, and furthermore, it contains small pre-factor $\cos 2\theta/4 \sim 0.1$. It is for this reason the correction is rather small in spite of large values of η. However, convergence of the series is determined by η itself, and so, the corrections to the first order ΔP_{osc} are not small. Although (2.16) allows to understand the size of the correction, in our estimations we use exact expression for $\cos^2\theta^0_m$. In the limit of small η the depth of oscillations

$$A_P \approx \sin^2 2\theta\ \eta \tag{2.17}$$

decreases linearly, that is, slower than correction to the average value.

In fig. 2 the averaged survival probability is shown as a function of the neutrino energy for different production points (different initial densities). The shadowed strips show the depth which oscillations would have at the surface of the Sun, provided that there is no loss of coherence. The average P converges to $P_{non-osc}$ (dashed line) with increase of energy and ρY_e. The decrease of oscillation depth with η is much slower than convergence of P to $\sin^2\theta$: $\Delta P \propto \eta^2$, $A_P \propto \eta$. The depth of oscillations increases with decrease of E approaching the vacuum value. Notice that even for the highest energies of the spectrum the conversion is not completely non-oscillatory, though $P \approx \sin^2\theta$.

At low energies ($E < 2$ MeV) the Earth regeneration ($\propto (\Delta m^2/E)^2$) can be neglected and the probability is given by the vacuum oscillation formula with small matter corrections. For $\eta \gg 1$ we can write:

$$P \approx P_{vac} - \frac{1}{2\eta}\cos 2\theta \sin^2 2\theta. \tag{2.18}$$

For the beryllium neutrinos the effective density in the production region $(\rho Y_e)_0 = 87$ g/cc, and correspondingly, $\eta = 6.28$. Inserting this value of η in (2.18) we find $\Delta P = -0.028$ which is smaller than 5% of P_{vac}.

For the *pp*-neutrinos the effective density in the region of the highest production rate is $(\rho Y_e)_0 \sim 68$ g/cc. At $E = 0.4$ MeV this gives $\eta = 17.3$ and correction $\Delta P = -0.01$.

The effect of the coherence loss of a neutrino state on the conversion picture has not been taken in to account here. The loss of coherence suppresses depth of oscillations, so that the probability converges to the average value (see [19]).

3. What is next

Next step in developments of the field will include

- further checks of the LMA solution, searches for signatures of solution (day-night asymmetry, distortion of spectrum), consistency checks;
- precision measurements of the oscillation parameters Δm^2_{12}, $\sin^2\theta_{12}$;
- searches for physics beyond LMA, sub-leading effects: effects of 1 - 3 mixing, spin-flavor precession, new neutrino interaction, searches for sterile neutrinos;
- precise determination of the solar neutrino fluxes, astrophysics of the Sun
- checks of CPT, equivalence principle, etc..

Let us consider first predictions for the forthcoming experiments.

1). SNO spectrum. Distortion of the energy spectrum is the generic consequence of the LMA MSW solution. As we discussed in the previous section, with decrease of energy the survival probability increases due to increase of the oscillation contribution.

In fig. 3 we show the results of calculations of spectra for different values of Δm^2. The distortion due to oscillations which dominates at low energies is partly compensated by the regeneration effect at high energies. Thus, for the day signal one expects stronger upturn.

According to fig. 3, the upturn is about 8 - 15%. We show also the SNO experimental points from the salt phase. A dependence of the distortion on Δm^2 is rather weak in the allowed region. Notice that in the low energy part the spectrum has a tendency to turn down in contrast to the expected effect. At $E < 7.5$ MeV the points are systematically below the predicted rate. One should notice, however, that the experimental points include the statistical error only and it is not excluded that some systematics explains the observed result.

2). KamLAND: rate versus spectrum. More precise measurements of the rate and spectrum distortion are expected. That can further diminish uncertainty in the determination of Δm^2. In fig. 4 we show the contours of constant suppression of the KamLAND rate R_{KL} above 2.6 MeV:

$$R_{KL} \equiv \frac{N(\Delta m^2, \tan^2\theta)}{N_0}, \tag{3.1}$$

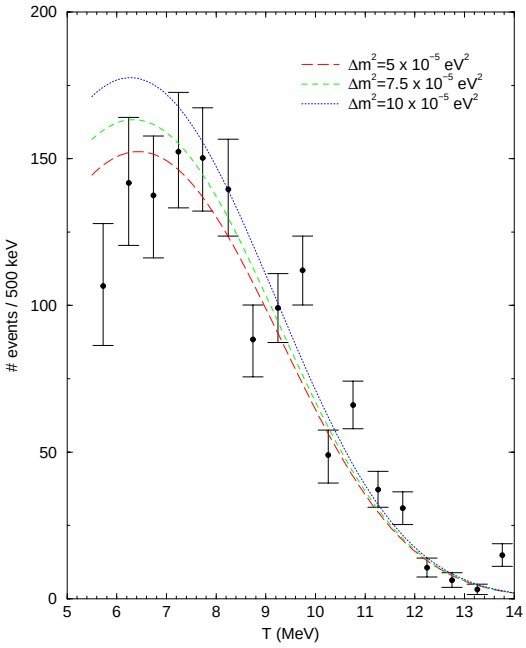

Figure 3: The energy spectrum of the CC reaction events. Shown is the distribution of events in the kinetic energy for different values of Δm^2 and $\tan^2\theta = 0.39$. We show also the SNO experimental points from the salt phase.

where N and N_0 are the numbers of events with and without oscillations. As follows from the figure strengthening of the lower bound on R_{KL} will cut the allowed region from the side of small Δm^2 ($\sim 5\cdot 10^{-5}$ eV^2) as well as large Δm^2 ($\sim 9\cdot 10^{-5}$ eV^2) and large mixings: $\tan^2\theta \sim 0.45$. In contrast, strengthening of the upper bound on R_{KL} will disfavor the region of small mixings: $\tan^2\theta \sim 0.3$.

The spectrum distortion can be characterized by a relative suppression of rates at the high and low energies. We choose $E = 4.3$ MeV as the border line [20], so that the interval (2.6 - 4.3) MeV contains 4 energy bins. Introducing the rates $R_{KL}(< 4.3$ MeV) and $R_{KL}(> 4.3$ MeV) we define the *shape parameter* as

$$k = \frac{1 - R_{KL}(> 4.3 \text{ MeV})}{1 - R_{KL}(< 4.3 \text{ MeV})}. \tag{3.2}$$

k does not depend on the normalization of spectrum and on the mixing angle in the 2ν context. It increases with the oscillation suppression of signal at high energies. $k > 1$ ($k < 1$) means stronger suppression at high (low) energies. The present KamLAND data give [20]

$$k^{exp} = 0.84^{+0.42}_{-0.35}, \quad 1\sigma. \tag{3.3}$$

In fig. 4 we show the contours of constant shape parameter. According to this figure at the 1σ level

$$k^{th} = 1.05^{+0.75}_{-0.50} \tag{3.4}$$

in a very good agreement with (3.3). In the l-LMA (1σ) region we find $k = 0.5 - 2.3$. So that even mild increase of statistics will influence the allowed range of Δm^2.

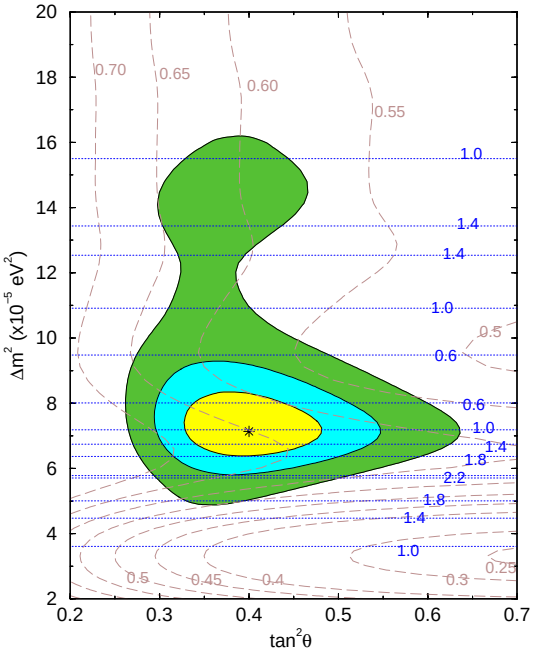

Figure 4: The contours of constant rate suppression, R_{KL} (dotted) and the spectrum shape parameter k (dashed) at KamLAND. We show also the allowed regions of the oscillation parameters from the combined fit of the solar neutrino data and the KamLAND spectrum. The best fit point is indicated by a star.

In the h-LMA region the allowed interval, $k = 0.9 - 1.4$, is narrower. So, if forthcoming measurements favor $k < 0.9$ or $k > 1.4$, the h-LMA region will be further discriminated.

3). SNO CC/NC *ratio versus the Day-night asymmetry.* In fig. 5 we show the contours of constant CC/NC ratio with finer grid than before. We find predictions for the best fit point and the 3σ interval:

$$\frac{\text{CC}}{\text{NC}} = 0.32^{+0.08}_{-0.07} \ , \quad (3\sigma). \tag{3.5}$$

In fig. 5 we show also the contours of constant A_{DN}^{SNO} for the energy threshold 5.5 MeV. The best fit point prediction and the 3σ bound equal

$$A_{ND}^{SNO} = 3.0 \pm 0.8\% \ , \quad (1\sigma), \qquad A_{ND}^{SNO} < 6\% \quad (3\sigma). \tag{3.6}$$

4). Germanium versus Clorine production rates. In the best fit point we predict $Q_{Ge} = 71$ SNU. We show in fig. 5 the lines of constant Ge production rate with finer (than before) grid.

For the Argon production we have $Q_{Ar} = 2.96$ SNU in the global b.f. point. We show in fig. 5 also the lines of constant Argon production rate.

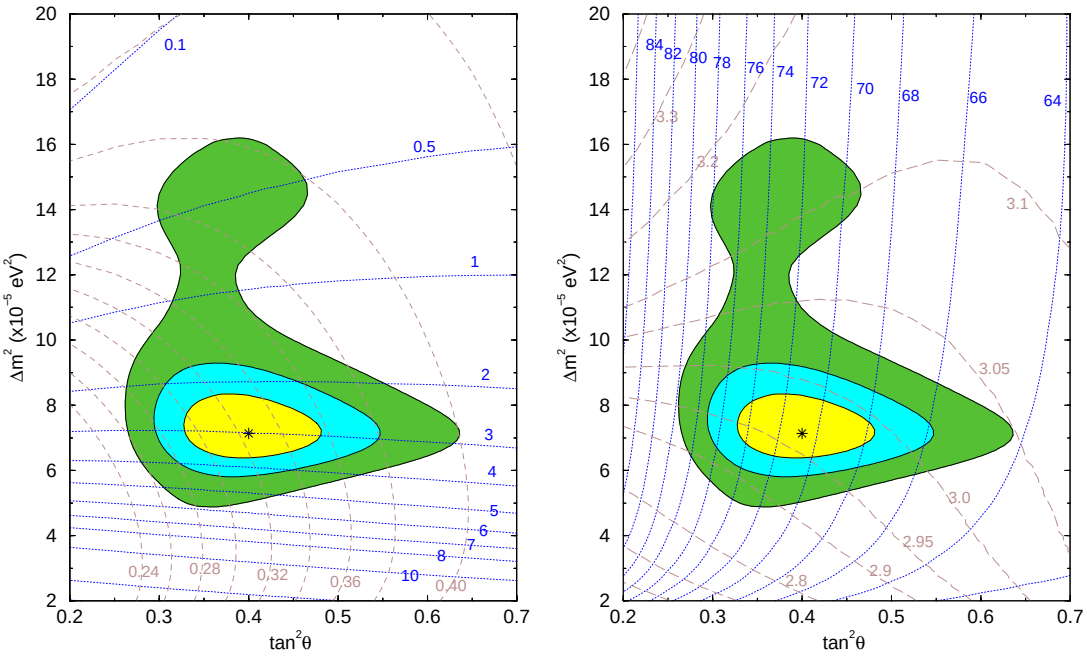

Figure 5: Predictions for the CC/NC ratio and the Day-Night asymmetry at SNO (left). The dashed lines are the lines of constant CC/NC ratio (numbers at the curves) and the dotted lines show the lines of constant A_{DN}^{SNO} (numbers at the curves in %). Predictions for the Germanium and Argon production rates (right). The dotted lines are the lines of constant Germanium production rate, Q_{Ge}, and the dashed lines show the lines of constant Argon production rate ,Q_{Ar} (numbers at the curves in SNU), in the $\Delta m^2 - \tan^2\theta$ plane. We show also the 1σ and 3σ allowed regions of the oscillation parameters from the combined fit of the solar neutrino data and the KamLAND spectrum. The best fit point is indicated by a star.

4. Beyond LMA

Is the LMA solution complete? If there are observations which may indicate some deviation from LMA?

4.1 Homestake result and sterile neutrinos

According to the recent analysis, LMA MSW describes all the data very well: pulls of predictions from experimental results are below 1σ for all but the Homestake experiment. The generic prediction of LMA for the Ar production rate is

$$Q_{Ar} = 2.9 - 3.1 \ \ \text{SNU}, \tag{4.1}$$

which is about 2σ higher than the Homestake result [6]. This pull can be

- just a statistical fluctuation;
- some systematics which may be related to the claimed long term time variations of the Homestake signal [6];
- a consequence of higher fluxes predicted by the Standard Solar Model (SSM) [2]

- some physics beyond LMA.

Another generic prediction of LMA is the "upturn" of the energy spectrum at low energies (the upturn of ratio of the observed and the SSM predicted numbers of events). According to LMA, the survival probability should increase with decrease of energy below (6 - 8) MeV. For the best fit point the upturn can be as large as 10 - 15 % between 8 and 5 MeV [24, 19]. Neither Super-Kamiokande (SK) [10] nor SNO [1] show the upturn, though the present sensitivity is not enough to make statistically significant statement.

There are also claims that the solar neutrino data have time variations with small periods [25]. If true, this can not be explained in the context of LMA solution.

Are these observations related? Do they indicate some new physics in the low energy part of the solar neutrino spectrum? Both the lower Ar-production rate and the absence of (or weaker) upturn of the spectrum can be explained by the effect of new (sterile) neutrino. The solar neutrino conversion in the non-trivial 3ν- context (when the effect of third neutrino is not reduced to the averaged oscillations) have been considered in a number of publications before [4, 26]. In particular, modification of the ν_e- survival probability due to the mixing with sterile neutrino has been studied [27]. We suggest [28] specific parameters of the sterile neutrino which lead to appearance of a dip in the adiabatic edge of the survival probability "bath", at $E = (0.5 - 2)$ MeV, and/or flattening of the spectrum distortion at higher energies $(2 - 8)$ MeV.

Let us consider the system of two active neutrinos, ν_e and ν_a, and one sterile neutrino, ν_s, which mix in the mass eigenstates ν_1, ν_2 and ν_0:

$$\begin{aligned} \nu_0 &= \cos\alpha\ \nu_s + \sin\alpha(\cos\theta\ \nu_e - \sin\theta\ \nu_a), \\ \nu_1 &= \cos\alpha\ (\cos\theta\ \nu_e - \sin\theta\ \nu_a) - \sin\alpha\ \nu_s, \\ \nu_2 &= \sin\theta\ \nu_e + \cos\theta\ \nu_a\ . \end{aligned} \tag{4.2}$$

The states ν_e and ν_a are characterized by the LMA oscillation parameters, θ and Δm^2_{12}. They mix in the mass eigenstates ν_1 and ν_2 with the eigenvalues m_1, and m_2. The sterile neutrino is mainly present in the mass eigenstate ν_0 (mass m_0). It mixes weakly ($\sin\alpha \ll 1$) with active neutrinos in the mass eigenstate ν_1. We will assume first that $m_2 > m_0 > m_1$ and consider the oscillation parameters of ν_s in the intervals:

$$\Delta m^2_{01} = m^2_0 - m^2_1 = (0.2 - 2) \times 10^{-5}\ \ \mathrm{eV}^2, \qquad \sin^2 2\alpha \sim 10^{-5} - 3 \cdot 10^{-3}. \tag{4.3}$$

Let ν_{1m}, ν_{2m}, ν_{0m} be the eigenstates, and λ_1, λ_2, λ_0 the corresponding eigenvalues of the 3ν-system in matter. We denote the ratio of mass squared differences as

$$R_\Delta \equiv \frac{\Delta m^2_{01}}{\Delta m^2_{21}}. \tag{4.4}$$

4.2 Survival probability. Properties of the dip

The survival probability is given by

$$P_{ee} \equiv |\langle \nu_e | \nu_f \rangle|^2 \approx \sin^2\theta^0_m \sin^2\theta + \cos^2\theta^0_m \cos^2\theta \left[\cos^2\alpha^0_m - P_2 \cos 2\alpha^0_m\right], \tag{4.5}$$

where θ^0_m and α^0_m are the mixing angles in matter in the neutrino production point, P_2 is the two neutrino jump probability in the system $\nu_{1m} - \nu_s$. Here we have neglected a small admixture of ν_e in ν_0: $\langle \nu_e | \nu_0 \rangle \approx 0$. Also we have taken into account that the coherence of the mass eigenstates is destroyed on the way from the Sun to the Earth due to a spread of the wave packets and averaging effects.

Similarly we obtain the transition probability of the electron to sterile neutrino:

$$P_{es} \equiv |\langle \nu_s | \nu_f \rangle|^2 \approx \cos^2 \theta^0_m \left[\sin^2 \alpha^0_m + P_2 \cos 2\alpha^0_m \right] . \tag{4.6}$$

In fig. 6 we show results of numerical computations of the ν_e survival probability P_{ee}, and the survival probability of active neutrinos, $(1 - P_{es})$, as functions of energy. In our numerical calculations we have performed a complete integration of the evolution equations for the 3ν-system and also made averaging over the production region of the Sun.

The effect of s-mixing is reduced to appearance of a dip in the LMA energy profile. A size of the dip equals:

$$\Delta P_{ee} \equiv P^{LMA}_{ee} - P_{ee} = P_{es} \cos^2 \theta, \tag{4.7}$$

where $P_{ee}(E)^{LMA} = P_{ee}(E)^{adiab}$ is the LMA probability given by the adiabatic formula (4.5). Since $\cos^2 \theta < 1$ (the best fit value of LMA mixing, $\cos^2 \theta = 0.714$) according to (4.7) a change of the ν_e survival probability due to mixing with ν_s is weaker than the transition to sterile neutrino P_{es}. The relation (4.7) is well reproduced in fig. 6.

The maximal suppression in the dip depends on R_Δ and α. For small R_Δ (large spit between the two resonances) and large α ($\sin^2 2\alpha > 10^{-3}$) the absolute minimum

$$P_{min} = P_{ee} \approx \sin^4 \theta \ . \tag{4.8}$$

can be achieved. The condition for the minimum is nearly satisfied for the solid line in the upper panel of fig. 6 where $P_{ee} \sim 0.1$.

With increase of R_Δ (smaller split of the resonances) or/and decrease of α (stronger violation of the adiabaticity) a suppression in the dip weakens. Also with decrease of α the dip becomes narrower.

4.3 Three scenarios

Three phenomenologically different scenarios can be realized depending on the oscillation parameters, and therefore on the position and form of the dip. Three panels in the fig. 7, which correspond to different values of R_Δ, illustrate these scenarios. Let us describe features of these three possibilities.

1). Narrow dip at low energies: the Be-line is in the dip. This corresponds to $\sin^2 2\alpha < 10^{-4}$ and $R_\Delta < 0.08$ or

$$0.5 E_{Be} < E_s(n_c) < E_{Be}, \tag{4.9}$$

where $E_{Be} = 0.86$ MeV is the energy of the Be-neutrinos (first panel in fig. 6 and solid line in fig. 7). The lower bound (4.9) implies that the pp-neutrino flux is not affected. In this case the Be-line is suppressed most strongly; the ν_e fluxes of the intermediate energies (pep and CNO neutrinos) are suppressed weaker and the low energy part of the boron neutrino spectrum measured by SK and SNO is practically unaffected.

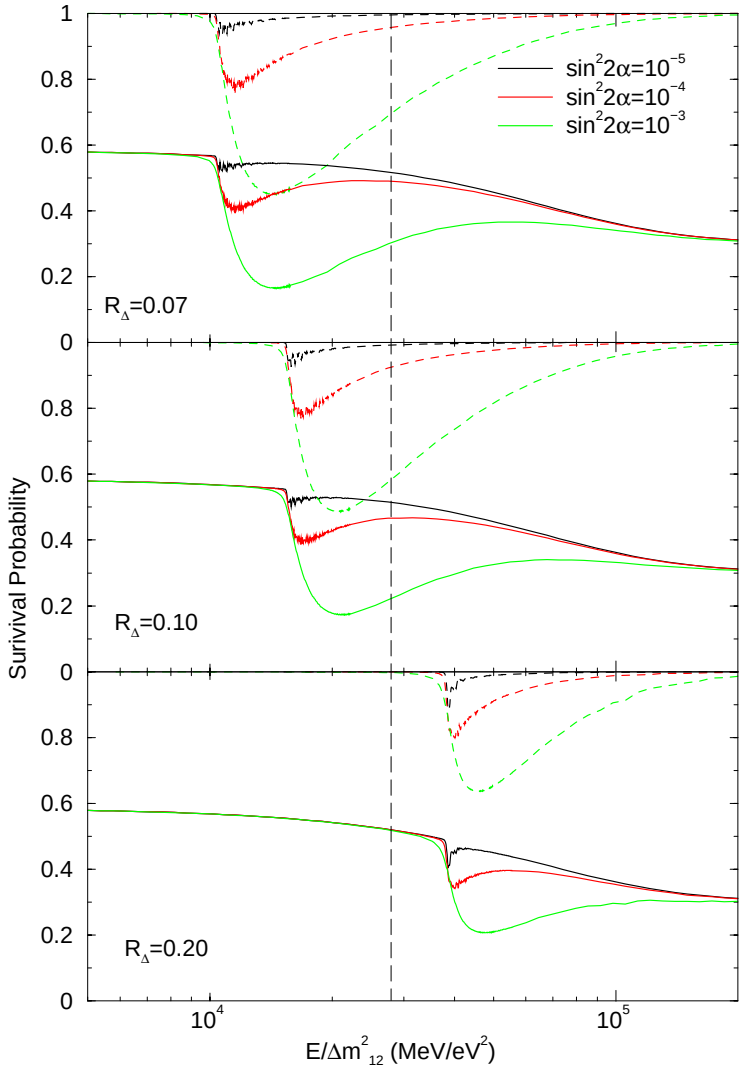

Figure 6: The survival probability of the electron neutrinos, P_{ee}, (solid line) and survival probability of the active neutrinos, $1 - P_{es}$, (dashed line), as functions of $E/\Delta m^2_{12}$ for different values of the sterile-active mixing parameter $\sin^2 2\alpha$. We take $\tan^2\theta = 0.4$. Also shown is position of the 1-2 resonance for the central density of the Sun. (vertical dashed line).

Taking the present 1σ errors, 0.23 SNU and 5 SNU, for the Homestake and the combined Gallium result correspondingly, we find that the central experimental value of Q_{Ar} can be reached at the price of the 2σ decrease of Q_{Ge}.

The best compromise solution would correspond to $\sin^2 2\alpha \sim 7 \cdot 10^{-5}$, when Q_{Ar} is 1σ above the observation, and Q_{Ge} is 1σ below the observation. In this case the BOREXINO rate reduces from 0.61 down to 0.48 of the SSM rate (see sect. 4.4).

For $E_s(n_c)$ being substantially smaller than E_{Be}, the Be- line is on the non-adiabatic edge of the dip and its suppression is weaker. In this case larger values of $\sin\alpha$ are allowed.

As we have discussed in sec.4 variations of the LMA parameters and the original boron

neutrino flux do not allow us to compensate completely the changes of the observables (which worsen the fit) in the case when the Be-line is suppressed.

2). The dip at the intermediate energies:

$$E_{Be} < E_s(n_c) < 1.4 \text{ MeV} \tag{4.10}$$

(see the second panel in fig. 6 and the dashed lines in fig. 7). The Be-line is out of the dip and therefore unaffected. A decrease of Q_{Ar} occurs due to suppression of the ν_e components of the *pep*- and CNO- neutrino fluxes.

In this case a decrease of Q_{Ar} is accompanying by smaller decrease of Q_{Ge} in comparison with the previous case. Now the value $Q_{Ar} = 2.8$ SNU, which is 1σ above the observation, can be achieved by just 0.4σ reduction of Q_{Ge}.

The BOREXINO signal due to the Be- flux is unchanged, and also the observable part of the boron neutrino flux is affected very weakly. Change of the CC/NC ratio is about 0.002.

The optimal fit (see fig. 7) would correspond to $\sin^2\alpha = 10^{-3}$, when Q_{Ar} is diminished down to 2.75 SNU, at the same time $Q_{Ge} = 68$ SNU and CC/NC = 3.22 in agreement with the latest data [1].

3). The dip at high energies:

$$E_s(n_c) > 1.6 \text{ MeV} \tag{4.11}$$

(see fig. 6, the panel for $R_\Delta = 0.2$, and the dotted lines in fig. 7). Q_{Ar} is diminished due to suppression of the low energy part of the boron neutrino spectrum. For $\sin^2\alpha = 10^{-3}$, we find $\Delta Q_{Ar} = 0.17$ SNU. At the same time a decrease of the Ge-production rate is very small: $\Delta Q_{Ge} \sim 0.5$ SNU.

At $\sin^2\alpha = 10^{-3}$ there is already significant modification of the observable part of the boron neutrino spectrum and decrease of the total rate at SK and SNO. Also the CC/NC ratio decreases. According to fig. 7 at $\sin^2 2\alpha = 10^{-3}$, we have $\Delta(\text{CC/NC}) = 0.01$. Further increase of R_Δ will shift the dip to higher energies, where the boron neutrino flux is larger. This, however, will not lead to further decrease of Q_{Ar} since the dip becomes smaller approaching the non-oscillatory region (see fig. 6). The BOREXINO signal (Be-line) is unchanged. So, the main signature of this scenario is a strong suppression of the upturn and even a possibility to bend the spectrum down.

Even for large R_Δ the influence of ν_s on the KamLAND results is negligible due to very small mixing. In contrast to the solar neutrinos, for the KamLAND experiment the matter effect on neutrino oscillations is very small and no enhancement of the s-mixing occurs. Therefore the effect of s-mixing on oscillation probability is smaller than $\sin^2 2\alpha \sim 10^{-3}$. For this reason the KamLAND result has not been included in the fit of data.

4.4 Further tests

How one can check the described scenarios?

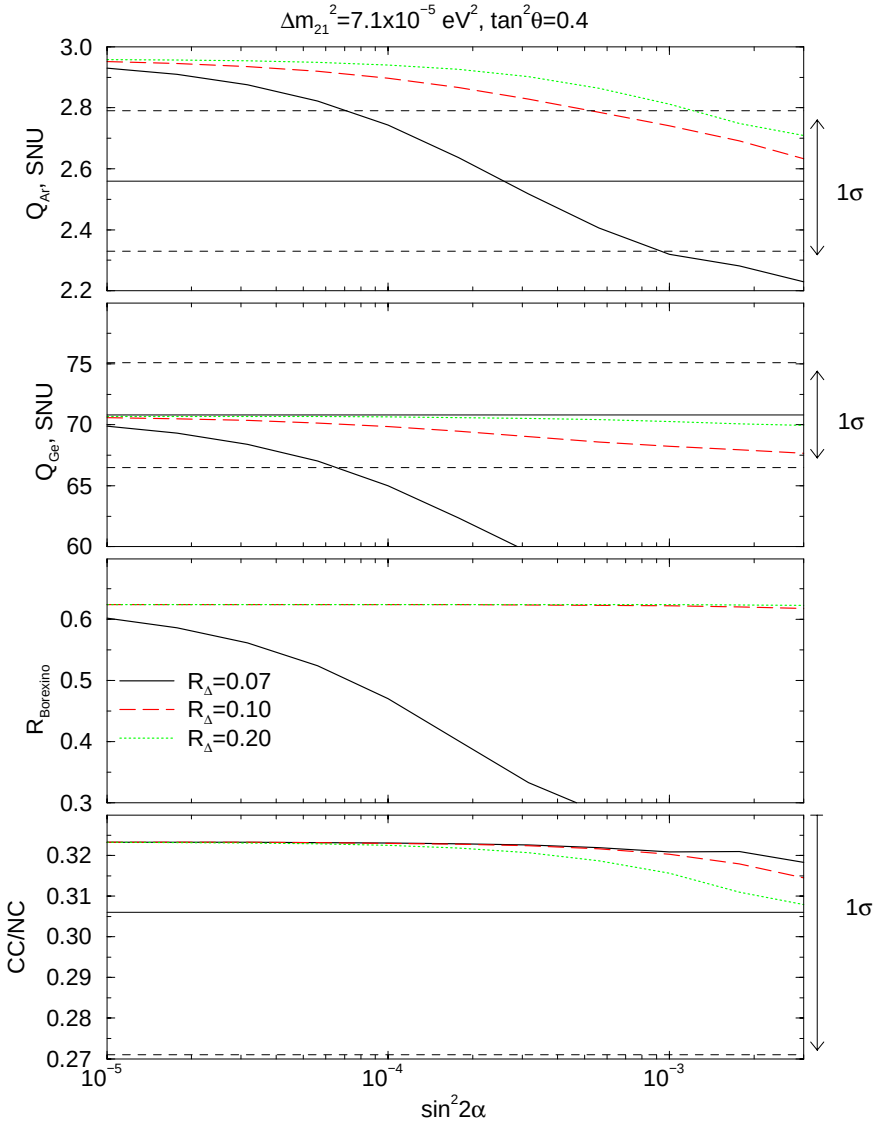

Figure 7: The Ar production rate (upper panel), the Ge production rate (second panel) the suppression factor for the BOREXINO signal and the CC/NC ratio at SNO as functions of $\sin^2 2\alpha$, for $\tan^2\theta = 0.4$ and $\Delta m^2_{21} = 7.1 \times 10^{-5}$ eV^2.

1) BOREXINO and KamLAND (solar) as well future low energy experiments [30, 31, 32, 33, 34, 35, 36] can establish the suppression of the Be-neutrino flux in comparison with the LMA predictions, if the case 1) is realized. In BOREXINO and other experiments based on the νe-scattering the ratio of the numbers of events with and without conversion can be written as

$$R_{Borexino} = P_{ee}(1 - r) + r - rP_{es}, \tag{4.12}$$

where $r \equiv \sigma(\nu_\mu e)/\sigma(\nu_e e)$ is the ratio of cross-sections. Using Eq. (4.7) we find an additional suppression of the BOREXINO rate in comparison with the pure LMA case:

$$\Delta R_{Borexino} \equiv R^{LMA}_{Borexino} - R_{Borexino} = (1 - r)\Delta P_{ee} + rP_{es} \approx \Delta P_{ee}(1 + r\tan^2\theta). \tag{4.13}$$

According to fig. 7, $R^{LMA}_{Borexino}$ can be diminished rather significantly. However, if the prediction for Q_{Ge} is 2σ (or less) below the experimental results, we find $R^{LMA}_{Borexino} > 0.4$ and $\Delta R_{Borexino} < 0.2$. For the best fit value in the scenario 1):

$$R^{LMA}_{Borexino} \sim 0.5, \quad (\Delta R_{Borexino} \sim 0.1). \tag{4.14}$$

Clearly, it will be difficult to establish such a difference. Furthermore, an additional suppression is mainly due to conversion to the sterile neutrino and the problem is to distinguish the conversion effect and lower original flux: the CC/NC ratio can not be used. Therefore not only high statistics results but also precise knowledge of the original fluxes is needed. The *pep*-flux is well known, however predictions of the CNO neutrino fluxes have larger uncertainties.

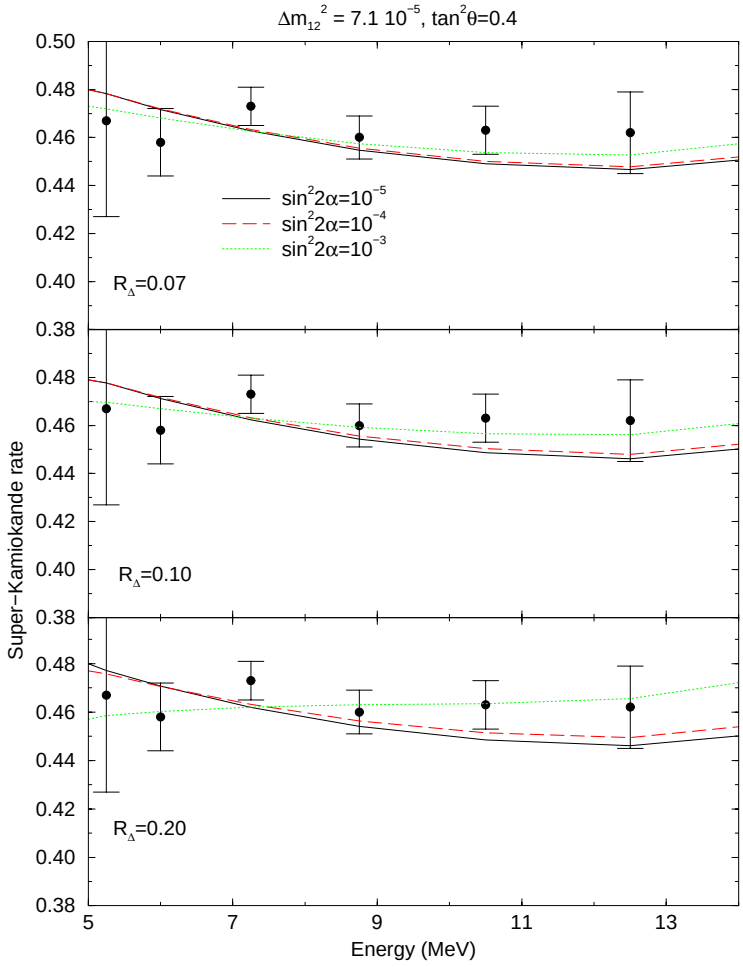

Figure 8: The spectrum distortion at Super-Kamiokande (N^{osc}/N^{SSM}) for different values of the sterile-active mixing parameter $\sin^2 2\alpha$ and the mass ratio R_Δ. Normalization of spectra have been chosen to minimize χ^2 fit of spectrum. We show also the Super-Kamiokande experimental data points (statistical errors only).

2). It may happen that the dip is at higher energies and the Be- flux is unaffected. In this case one expects significant suppression of the *pep*- and CNO- fluxes. Such a

possibility can be checked using combination of measurements from different experiments which are sensitive to different parts of the solar neutrino spectrum. The radiochemical *Li*- experiment [37] has high sensitivity to the *pep*- and *CNO*- neutrino fluxes [38].

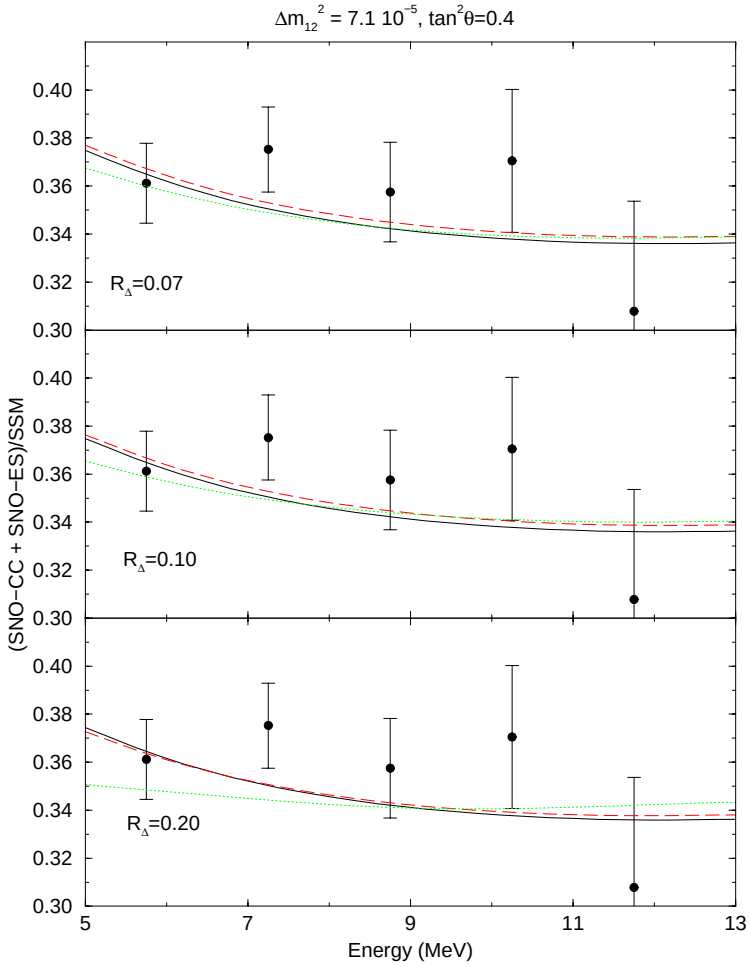

Figure 9: The spectrum distortion at SNO ($N^{osc}_{CC+ES}/N^{SSM}_{CC+ES}$) for different values of the sterile-active mixing parameter $\sin^2 2\alpha$ and the mass ratio R_Δ. Normalization of spectrum (for each parameter set) has been chosen to minimize χ^2 fit of spectrum. We show also the SNO experimental points with statistical errors only. The number of experimental points is reduced by combining results from three sequent energy bins.

Precise measurements of Q_{Be} and Q_{Ge} and independent measurements of the B, pp and Be neutrino fluxes and subtraction of their contributions from Q_{Be} and Q_{Ge} will allow to determine the CNO- electron neutrino fluxes. In general, to measure oscillation parameters and to determine the original solar neutrino fluxes one will need to perform a combined analysis of results from *Ga*-, *Cl*-, *Li*- experiments as well as the dedicated low energy experiments [30, 31, 32, 33, 34, 35, 36]. Of course, new high statistics *Cl*-experiment would clarify the situation directly.

3). For $R_\Delta \sim 0.1 - 0.2$ and $\sin^2 2\alpha \sim 10^{-3}$ one expects significant suppression of the low energy part of the B- neutrino spectrum. As follows from figs. 8 and 9, at 5 MeV an

additional suppression due to sterile neutrino can reach (10 - 15)% both in SK and SNO. The spectra with the s-mixing give slightly better fit to the data. Notice that there is no turn down of the SNO spectrum for $R_\Delta = 0.2$ and $\sin^2\theta_{13} = 10^{-3}$ due to an additional contribution from the $\nu - e$ scattering. Precision measurements of shape of the spectrum in the low energy part ($E < 6 - 8$ MeV) will give crucial checks of the described possibility.

4). In supernovae, neutrinos are produced at densities far above the LMA resonance density and propagation is adiabatic in the LMA resonance. So, even for very small 1-3 mixing ($\sin^2\theta_{13} > 10^{-4}$) the adiabatic conversion $\nu_e \to \nu_2$ is realized without any effect of sterile neutrino. If, however, the sterile level crosses the second level λ_2^{LMA} one may expect some manifestations of the sterile neutrino in the ν_e channel, provided that the mass hierarchy is inverted or the 1-3 mixing is very small ($\sin^2\theta_{13} < 10^{-4}$).

5). Smallness of mixing of the sterile neutrino allows one to satisfy the nucleosynthesis bound: such a neutrino does not equilibrate in the Early Universe. For this reason sterile neutrinos also do not influence the large scale structures formation in the Universe.

6). A very small s-mixing means that the width of s-resonance is also very small. In the density scale $\Delta n/n = \tan 2\alpha \sim 10^{-2}$. Therefore 1% density perturbations can strongly affect conversion in the s-resonance [39]. If density perturbations (or density profile) change in time, this will induce time variations of neutrino signals. Since the effect of s-resonance is small, one may expect 10% (at most) variations of the Ga- and Ar- production rates.

5. To the precision measurements in solar neutrinos. Effect of 1-3 mixing

Both for the KamLAND and for solar neutrinos the oscillations driven by Δm^2_{13} are averaged out and signals are determined by the survival probabilities

$$P_{ee} = (1 - \sin^2\theta_{13})^2 P_2 + \sin^4\theta_{13} \approx (1 - 2\sin^2\theta_{13})P_2, \tag{5.1}$$

where $P_2 = P_2(\Delta m^2_{12}, \theta_{12})$ is the two neutrino vacuum oscillation probability in the case of KamLAND and it is the matter conversion probability in the case of solar neutrinos.

The effect of non-zero 1- 3 mixing is reduced to the overall suppression of the survival probability. According to recent analysis of the atmospheric neutrino data [40] the allowed region of oscillation parameters has shifted to smaller Δm^2_{13}, and consequently, the upper bound on 1-3 mixing from the CHOOZ experiment [41] becomes weaker: $\sin^2\theta_{13} = 0.067$ (3σ) [42]. For this value of $\sin^2\theta_{13}$, the suppression can reach 13% in (5.1). The influence of $\sin^2\theta_{13}$ on the global fit can be traced in the following way.

There are three sets of observables for which effects of $\sin^2\theta_{13}$ are different.

1) Total rates (fluxes) at high energies measured by SNO and SK. These rates depend essentially on the combination $\cos^4\theta_{13}P_2$. In particular,

$$\frac{\mathrm{CC}}{\mathrm{NC}} \approx \cos^4\theta_{13}P_2, \qquad \frac{\mathrm{ES}}{\mathrm{NC}} \approx \cos^4\theta_{13}P_2(1 - r) + r. \tag{5.2}$$

The ratios of fluxes are unchanged if

$$\cos^4\theta_{13}\langle P_2(\Delta m^2_{12}, \tan^2\theta_{12})\rangle = const., \tag{5.3}$$

where $\langle ... \rangle$ is the averaging over the relevant energy range. The product (5.3) is invariant with increase of $\sin^2\theta_{13}$ (decrease of $\cos^4\theta_{13}$) if the probability increases. In the region near the b.f. point (1.3) the latter requires increase of Δm^2_{12} or/and $\tan^2\theta_{12}$. Then the absolute values of fluxes can be reproduced by tunning f_B (in the free f_B fit).

With increase of $\sin^2\theta_{13}$ the predicted spectrum becomes flatter which does not change the quality of fit significantly.

The day-night asymmetry decreases with increase of Δm^2_{12} which is slightly disfavored by the data. Future more precise measurements of asymmetry will have stronger impact.

2) Low energy observables, sensitive to *pp*- and *Be*- neutrino fluxes. They depend on the averaged vacuum oscillation probability. In particular, the Ge-production rate is proportional to

$$Q_{Ge} \propto \cos^4\theta_{13}(1 - 0.5\sin^2 2\theta). \tag{5.4}$$

Notice that practically there is no dependence of these observables on Δm^2_{12}. Since in the best fit point for zero 1-3 mixing $Q_{theor} \approx Q_{exp}$, a significant increase of $\sin^2\theta_{13}$ will lead to worsening of the fit (though small non-zero 1-3 mixing, $\sin^2\theta_{13} < 0.04$, could be welcomed).

3) KamLAND. The present best fit point is near the maximum of oscillation survival probability averaged over the atomic reactors. So, the increase of 1-3 mixing could be compensated by the decrease of 1-2 mixing.

These features allow one to understand results of the data fit.

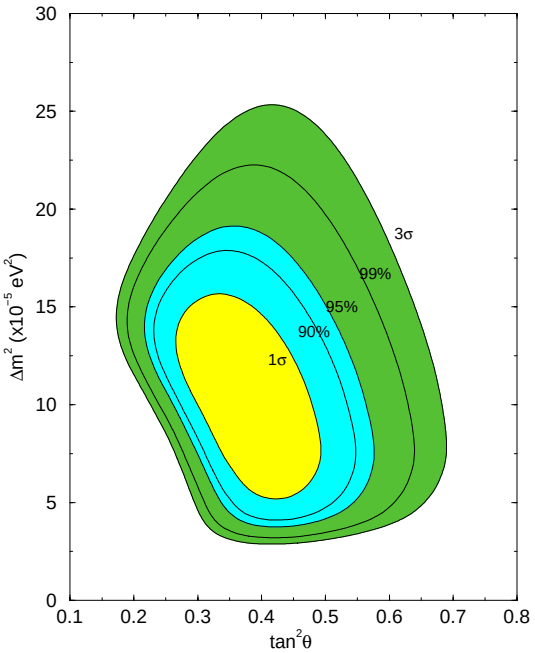

Figure 10: Three neutrino analysis with $\sin^2\theta_{13} = 0.067$. The allowed regions in $\tan^2\theta - \Delta m^2$ from a combined fit of the solar neutrino data at the 1σ, 90%, 95%, 99% and 3σ C.L..

We have performed analysis of the solar neutrino data for fixed value $\sin^2\theta_{13} = 0.067$

(fig. 10). The best fit point

$$\Delta m^2 = 11.0 \cdot 10^{-5}\text{eV}^2, \quad \tan^2\theta = 0.38, \quad f_B = 1.03 \tag{5.5}$$

corresponds to $\chi^2/d.o.f. = 66.8/81$. It is shifted to larger Δm^2 to satisfy condition (5.3). The shift to larger 1-2 mixing is disfavored by the Gallium experimental results (5.4). The allowed region is also shifted to larger Δm^2 and its size increases (also in the mixing direction). These results agree with the analysis in [15].

6. Conclusions

1). The improvements in measurements of the oscillation parameters lead to a situation when physics of the solar neutrino conversion is essentially (and quantitatively) determined.

2). The low (with respect to the LMA prediction) value of the Ar-production rate measured in the Homestake experiment and/or suppressed upturn of the spectrum at low energies in SK and SNO can be explained by introduction of the sterile neutrino which mixes very weakly with the active neutrinos.

3). After the SNO salt results the errors of determination of the oscillation parameters become smaller than the values of parameters:

$$\delta(\Delta m^2) < \Delta m^2, \quad \delta(\tan^2\theta) < \tan^2\theta. \tag{6.1}$$

This means that the solar neutrino studies enter a stage of precision measurements.

Acknowledgments

This work was supported by the TMR, EC-contract No. HPRN-CT-2000-00148 and No. HPRN-CT-2000-00152.

References

[1] SNO collaboration (Q. R. Ahmad *et al.*), nucl-ex/0309004.

[2] J. N. Bahcall, M.H. Pinsonneault and S. Basu, Astrophys. J. **555**, 990 (2001).

[3] L. Wolfenstein, Phys. Rev. **D 17**, 2369 (1978); L. Wolfenstein, in "Neutrino-78", Purdue Univ. C3 - C6, (1978).

[4] S. P. Mikheyev and A. Yu. Smirnov, Yad. Fiz. **42**, 1441 (1985) [Sov. J. Nucl. Phys. **42**, 913 (1985)]; Nuovo Cim. **C9**, 17 (1986); S. P. Mikheyev and A. Yu. Smirnov, ZHETF, **91**, (1986), [Sov. Phys. JETP, **64**, 4 (1986)] (reprinted in "Solar neutrinos: the first thirty years", Eds. J.N.Bahcall *et. al.*).

[5] SNO collaboration, Q. R. Ahmad *et al.*; *ibidem* **87**, 071301 (2001); ibidem **89**, 011301 (2002); *ibidem* **89**, 011302 (2002).

[6] B. T. Cleveland *et al.*, Astroph. J. **496**, 505 (1998).

[7] SAGE collaboration, J.N. Abdurashitov *et al.* Zh. Eksp. Teor. Fiz. **122**, 211 (2002) [J. Exp. Theor. Phys. **95**, 181 (2002)], astro-ph/0204245; V. N. Gavrin, Talk given at the VIIIth International conference on Topics in Astroparticle and Underground Physics (TAUP 03), Seattle, Sept. 5 - 9, 2003.

[8] GALLEX collaboration, W. Hampel *et al.*, Phys. Lett. B **447**, 127 (1999).

[9] GNO Collaboration, E. Belotti, Talk given at the VIIIth International conference on Topics in Astroparticle and Underground Physics (TAUP 03), Seattle, Sept. 5 - 9, 2003.

[10] Super-Kamiokande collaboration, S. Fukuda *et al.*, Phys. Rev. Lett. **86**, 5651 (2001); Phys. Rev. Lett. **86**, 5656 (2001), Phys. Lett. B **539**, 179 (2002).

[11] Super-Kamiokande collaboration, M. B. Smy et al., hep-ex/0309011.

[12] KamLAND collaboration, K. Eguchi *et al.*, Phys. Rev. Lett. **90**, 021802 (2003).

[13] A. B. Balantekin and H. Yüksel, hep-ph/0309079.

[14] G.L. Fogli, E. Lisi, A. Marrone, A. Palazzo, hep-ph/0309100.

[15] M. Maltoni, T. Schwetz, M. A. Tortola, J.W.F. Valle, hep-ph/0309130 (v.2).

[16] P. Aliani, V. Antonelli, M. Picariello, E. Torrente-Lujan, hep-ph/0309156.

[17] P. Creminelli, G. Signorelli, A. Strumia, hep-ph/0102234, v.5, Sept. 15 (2003).

[18] A. Bandyopadhyay, S. Choubey, S. Goswami, S. T. Petcov, D.P. Roy, hep-ph/0309174.

[19] P. C. de Holanda, A. Yu. Smirnov, hep-ph/0309299.

[20] P. C. de Holanda, A.Yu. Smirnov, JCAP **0302**, 001 (2003).

[21] P. C. de Holanda, A. Yu. Smirnov, Phys. Rev. **D66**, 113005 (2002).

[22] A.Yu. Smirnov, Invited talk at 10th International Workshop on Neutrino Telescopes, Venice, Italy, 11-14 Mar 2003, hep-ph/0305106.

[23] S. Nakamura *et. al*, Nucl. Phys. **A707**, 561 (2002).

[24] P.I. Krastev, A.Yu. Smirnov, Phys. Rev. **D65**, 073022 (2002).

[25] P.A. Sturrock, G. Walther and M. S. Wheatland, Astrophys. J. **491** , 409 (1997); *ibidem* **507**, 978 (1998); P.A. Sturrock and M. A. Weber, Astrophys. **J. 565**, 1366 (2002). P.A. Sturrock, astro-ph/0304148; hep-ph/0304106. P. A. Sturrock and M. A. Weber, Astrophys. J. **565**, 1366 (2002); A. Milsztajn, hep-ph/0301252; P. A. Sturrock, hep-ph/0304073; hep-ph/0304106. D. O. Caldwell and P. A. Sturrock, hep-ph/0305303.

[26] Incomplete list: T.K. Kuo, James Pantaleone, Phys. Rev. Lett. **57**, 1805 (1986), Phys. Rev. **D35** 3432 (1987), A. Yu. Smirnov, in proc. of the Int. Symposium on Neutrino Astrophysics "Frontiers of Neutrino Astrophysics", October 19-22 (1992) Takayama, Japan, Eds. Y. Suzuki and K. Nakamura, p.105., Q.Y. Liu, S.T. Petcov, Phys. Rev. **D56**, 7392 (1997), K.S. Babu, Q.Y. Liu, A. Yu. Smirnov, Phys. Rev. **D57**, 5825 (1998).

[27] V. Berezinsky, M. Narayan, F. Vissani, Nucl. Phys. **B658**, 254 (2003). P.C. de Holanda, A.Yu. Smirnov, hep-ph/0211264.

[28] P.C. de Holanda, A.Yu. Smirnov, hep-ph/0307266.

[29] BOREXINO collaboration, G. Alimonti, *et al.*, Astropart. Phys. **16** 073022 (2002).

[30] R.S. Raghavan, Phys. Rev. Lett. **78**, 3618 (1997).

[31] H. Ejiri et al., Phys.Rev. Lett. **85**, 2917 (2000).

[32] Y. Suzuki, Low Nu2 workshop, Tokyo 2000,
http://www-sk.icrr.u-tokyo.ac.jp/neutlowe/.

[33] B. Lanou, in Low Nu3 Heidelberg, Germany, http://www.mpi-hd.mpg.de/nubis/.

[34] D. N. McKinsey and J. M. Doyle, J. of Low Temp. Phys. **118** 153 (2000).

[35] G Bonvicini et al., hep-ex/0109199, hep-ex/0109032.

[36] C. Broggini, Low Nu3 Heidelberg, Germany, http://www.mpi-hd.mpg.de/nubis/.

[37] J. N. Bahcall, Phys. Lett., **13**, 332 (1964) V. A. Kuzmin and G. T. Zatsepin, Proc. Int. Conf on Cosmic Rays, Jaipur, India, 1965 paper Mu-Nu 36, p. 1023.

[38] See for recent discussion: A. Kopylov, V. Petukhov, hep-ph/0301016, hep-ph/0306148.

[39] P.I. Krastev, A.Yu. Smirnov, Mod. Phys. Lett. **A6**, 1001 (1991).

[40] Super-Kamiokande Collaboration, Y. Hayato, talk given at the HEP2003 International Europhysics Conference (Aachen, Germany, 2003), website: eps2003.physik.rwth-aachen.de .

[41] CHOOZ Collaboration, M. Apollonio *et al.*, Phys.Lett. **B466**, 415 (1999); Eur. Phys. J. , C **27**, 331 (2003).

[42] G.L. Fogli, E. Lisi, A. Marrone, D. Montanino A. Palazzo, A.M. Rotunno, hep-ph/0308055.